IJE TRANSACTIONS B: Applications Vol. 32, No. 11, (November 2019) 1559-1569

International Journal of Engineering

Journal Homepage: www.ije.ir

Experimental Investigation on Cyclic Behavior of Butterfly-shaped Links Steel Plate Shear Walls

H. Valizadeh[a], H. Veladi*[a], B. Farahmand Azar[a], M. R. Sheidaii[b]

[a] *Civil Engineering Faculty, Tabriz University, Tabriz, Iran*
[b] *Civil Engineering Department, Urmia University, Urmia, Iran*

P A P E R I N F O

Paper history:
Received 10 July 2019
Received in revised form 05 September 2019
Accepted 12 September 2019

Keywords:
Butterfly Link
Energy Dissipation
Ductility
Shear Capacity
Steel Plate Shear Wall

A B S T R A C T

An innovative type called "butterfly-shaped links steel plate shear wall (BLSPSW)" was proposed as a lateral load resisting system. In this novel system, by creating butterfly-shaped links in the four sides of the web plate, the lateral load resisting mechanism is not the development of a diagonal tension field on the web plate (similar to Conventional SPSWs), but the capacity of the system is determined by the shear strength of the links. Therefore, the geometric parameters of the link as initial design inputs affect predicting and controlling the stiffness and strength of the BLSPSW. Three experimental specimens were loaded to examine the behavior of the proposed system. The first one was the conventional steel plate shear wall (called SPSW-1), and two others prepared of the butterfly-shaped link steel plate shear wall (BLSPSW) with links that have been controlled by shear yield (SPSW-BL 80) and flexural yield (SPSW-BL 130). The experimental results showed that the stiffness and strength of the BLSPSW specimens can be controlled by the link geometry. Also, the BLSPSWs indicated desirable ductility up to 10 percent and high energy dissipation, even in small drifts compared to the SPSW-1. At last, the shear strength formulation of the butterfly fuses was used to determine the shear capacity of the BLSPSWs and compared with the experimental results.

***doi**: 10.5829/ije.2019.32.11a.07*

1. INTRODUCTION

Due to many financial losses and casualties that occur each year because of the earthquake and wind forces, researchers have always been trying to achieve a suitable structural system with minimal damage. Steel plate shear walls (SPSWs) have been recognized as a reliable lateral load-resisting system due to the desirable energy dissipation capacity, stable hysteresis behavior and high lateral stiffness [1, 2]. A conventional SPSW consists of a web plate (as an initial lateral load-resisting element), connected to vertical boundary elements (VBEs) and horizontal boundary elements (HBEs) [3]. In spite of the use of thick plates or stiffened web plates in the initial design of the steel plate shear walls to limit the out-of-plane buckling of the thin plate [4], post-buckling strength and the remarkable ductility of the thin plate was observed under the lateral load in subsequent studies [5, 6]. This post-buckling strength is the result of a mechanism called diagonal tension field action, which requires very stiff boundary elements for development in the entire web plate and to strength to lateral loads [7]. The diagonal tension field produces significant axial and flexural forces in the columns. Especially in multi-story structures, the design of the columns is challenging because of the high axial force and the high flexural moment [8]. The basis of the design of the conventional steel plate shear wall is based on the idealization of the plate in such a way that it can withstand the entire base shear. According to the ANSI / AISC 341-16 code [9], in the design of the steel plate shear wall, the thickness of the plate is determined based on the design force, then the boundary elements must be designed in such a way that they remain in the elastic region before the diagonal tension field in the plate reaches to the maximum capacity. Therefore, the code recommends expressions for the least stiffness of the boundary elements.

*Corresponding Author Email: *hveladi@tabrizu.ac.ir* (H. Veladi)

Please cite this article as: H. Valizadeh, H. Veladi, B. Farahmand Azar, M. R. Sheidaii, Experimental Investigation on Cyclic Behavior of Butterfly-shaped Links Steel Plate Shear Walls, International Journal of Engineering (IJE), IJE TRANSACTIONS B: Applications Vol. 32, No. 11, (November 2019) 1559-1569

The conventional steel plate shear wall design method produces a system with a thin web plate and strong boundary elements that are not economical. This issue will be more evident in short and intermediate-range structures due to the need for an infill plate with a thickness corresponding to the operating condition (more than the thickness obtained from the design equations). Thus, up to now, different shapes of steel plate shear walls (SPSWs), such as perforated SPSWs [10, 11], light-gauge SPSWs [12], low yield point SPSWs [13], SPSWs with slits [14, 15], SPSWs with partially connected web plates [16], bound-columns with buckling-restrained SPSWs [17], buckling-restrained SPSWs with inclined-slots [18] have been proposed to reduce the stiffness of the boundary elements and improve the performance of the structural system. In the conventional steel shear walls, the only controllable parameter of the web plate is the slenderness factor which controls both parameters of the stiffness and the system's strength in a way that they reflect on each other. But having more initial design parameters for controlling stiffness and strength is considered as a strong point of the structural system. The purpose of this study is to develop an innovative type of lateral load-resisting system called "butterfly-shaped links steel plate shear wall (BLSPSW)" which prevents early elastic buckling of the web plate with proper thickness and by cutting the plate and creating butterfly links in the surrounding of the web plate. Elastic buckling is the main cause of pinching intensification and the drop of energy dissipation capacity in conventional steel plate shear walls. The load-resisting mechanism of BLSPSW is not the development of the diagonal tension field and is related to the shear capacity of the set of links. Therefore, the designer has more initial parameters to control the initial stiffness, strength, ductility, and energy dissipation capacity. The infill plate strength is a determinant factor in the cross-sectional dimension of the boundary element and reasonable and economical boundary elements can be obtained by controlling this factor.

2. BUTTERRFLY FUSE PLATE

A steel plate with a butterfly-shaped link (Figure 1) is a form of energy-dissipating structural fuse [19]. When the shear force is applied to it, the butterfly-shaped link can develop a controlled flexural yield. By tapering (a cone geometry), it is possible to control the yield point and delaying the fracture by distancing the plastic hinges from the link corners.

Eatherton et al. [20] utilized butterfly-shaped structural fuses for dissipation of seismic energy as part of a self-centering lateral load-resisting system in which the steel frame was rocking motion braced. El-Bahey and Bruneau [21] also used butterfly-shaped plates between

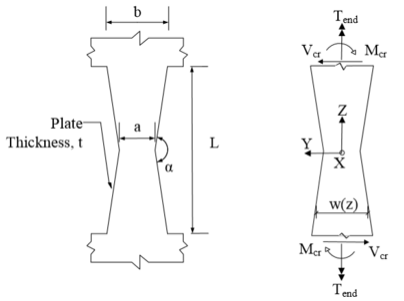

Figure 1. Butterfly fuse, geometry and internal forces [22]

the bridge pillars. One of the most practical design criteria is to create a good proportion in the butterfly links for initiation of the flexural yield in the distance of L/4 from the middle section and distancing the fracture from the two ends of the link. Ma et al. [19] reported the ratio a/b = 0.33 (the width of the middle section to the width of the end of the link section) for this purpose. Some researches have developed formulas for predicting the shear strength of the butterfly-shaped links by using plastic mechanism analysis and with the assumption of plastic hinges [22]. These formulas generally have not considered the effect of shear stress and haven't heeded the limitation for the cases when the shear yield controls the system. In most cases, the flexural yield is more favorable concerning the large yielded area and the significant ductility. However, shear yield can control the behavior of short links [22, 23].

Farzampor and Eatherton [22] described two flexure and shear limit states according to the link geometry for butterfly-shaped links. The flexure limit state occurs at the beginning of flexural yielding and the formation of plastic hinges at L/4 (L=length of the link) of the middle section and the limit state in shear indicates the beginning of the shear yield in the critical width of the link (the lowest cross-sectional area). Therefore, the shear capacity of the link is equal to the strength obtained from the first probable limit state according to the geometric shape of the link. They presented the following formulas for calculating the shear strength of the butterfly link according to the limit states which control the link behavior:

For flexural limit state Equations (1a) and (1b):

$$V_p^{flex} = 2\ at\ F_y \frac{(b-a)}{L}\ \ for\ \ {}^{a}/_{b} \le {}^{1}/_{2} \tag{1a}$$

$$V_p^{flex} = \frac{b^2 t\, F_y}{2L}\ \ for\ \ {}^{a}/_{b} > {}^{1}/_{2} \tag{1b}$$

For shear limit state Equation (2):

$$V_p^{shear} = \ at\ \frac{F_y}{\sqrt{3}} \tag{2}$$

The parameters a, b, L, t and F_y are the width of the middle section, the width of the end section, the length, thickness and yield stress of the link materials.

3. EXPERIMENTAL PROGRAM

The main objective of the experimental test is to investigate the behavior of the proposed steel plate shear wall with butterfly-shaped links under cyclic loading, which represents an ideal earthquake force. For this purpose, three one-third scaled specimens with one-bay and one-story was built and loaded at Urmia University Crisis Research and Management Center laboratory to study the cyclic behavior, evaluation of seismic parameters and the fracture modes of the proposed structural system.

3. 1. Test Specimens Figure 2 illustrates the experimental specimens made before applying the cyclic load. The first specimen was the conventional SPSW with a web plate with a thickness of 0.8 mm called SPSW-1. Two other specimens were considered with plates with a thickness of 2.95 mm and butterfly-shaped links. On each side of the panel, there were seven butterfly-shaped links were created by laser (Figure 2). These specimens were named "BL 130" and "BL 80" according to the length of the link, L, which has been 130 and 80 mm, respectively. The dimensions of the web plate were 970 x 970 mm from edge to edge of boundary elements (Figure 3). An L50x50x5 mm angle was used to connect to the web plate, which was connected to the boundary elements by an a3 fillet weld. The infill plate on each side was connected to the angle using 16 M12-8.8 bolts according to DIN standard. These bolts were pre-tensioned by torque meter according to mechanical specifications, up to 55% of its ultimate tension. Table 1 indicates the geometric characteristics of the specimens. The position of the parameters a, b and L is shown in Figure 1. According to the results of previous studies (taper ratio), a/b=0.33 was selected.

3. 2. Test Setup The laboratory setup of a rigid steel frame, lateral bracing and cyclic loading system has been illustrated in Figure 3. The boundary elements made of stiffened IPE200 with a web plate, have been connected as a hinged frame by an M30 bolt with 8.8 grade. The hinge frame has been connected to a rigid truss fixed on the floor of the laboratory.

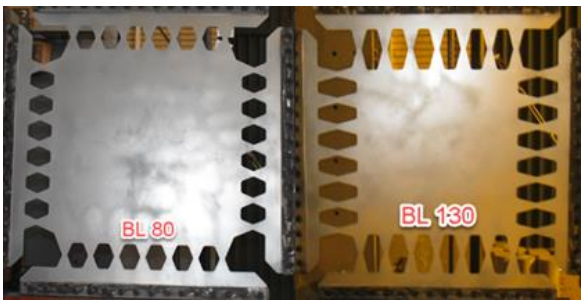

Figure 2. Laboratory specimens before loading

TABLE 1. Samples Geometric Specification

Sample	Thickness (mm)	L (mm)	a (mm)	b (mm)	Taper Ratio a/b	Slenderness Ratio L/t	Width Ratio b/L
SPSW-1	0.80	-	-	-	-	-	-
BL 80	2.95	80	16.5	50	0.33	27	0.62
BL 130	2.95	130	16.5	50	0.33	44	0.38

On the other side, it is attached to a girder connected to the loading hydraulic jack (Figure 3). Loads are applied to the frame upwards and downwards which represent tension and compressive by an actuator. The actuator capacity is 1000 kN for static loading and 600 kN for dynamic loading with a maximum loading speed of 60 mm/min. The girder which is connected to the jack is braced by the truss to brace lateral movements, so it is possible for the frame to have only one (vertical) degree of freedom.

3. 3. Instrumentation The displacement and equivalent load values were recorded in load cycles by the load cell and the displacement sensor connected to the actuator. This equipment, along with a data logger and Nene software, displays graphs of displacement-time, load-time, and load-displacement during loading. Also, three linear variable differential transformers (LVDTs) were used to measure displacement as follows: The LVDT 1 # for measuring the frame in the midpoint of the horizontal boundary element (to control the overall frame displacement), the LVDT 2 # for measuring the out-of-plane displacement of the frame and the LVDT 3 # for measuring the possible displacement of the rigid truss of the frame support. These LVDTs are connected to secondary data logger.

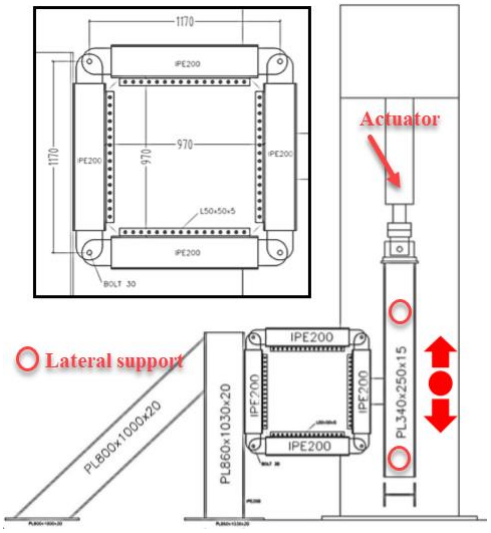

Figure 3. Specimen setup and loading system

3. 4. Material Properties To determine the mechanical properties of web plate materials, the tensile test was performed according to the ASTM E8 standard [24]. Two tensile specimens with a gauge length of 52 mm and thicknesses of 0.8 and 2.95 mm were prepared and tested. The mechanical properties of the specimens are presented in Table 2. The yield and ultimate stresses of the thinner plate, due to the cold rolling, are more than the other one.

3. 5. Displacement Protocol The specimens were subjected to quasi-static cyclic loading, starting from very small drift rates and were gradually added up to 5% according to the SAC loading protocol [25]. Figure 4 indicates the displacement protocol imposed on the specimen. According to this protocol, the specimen experiences displacements less than 1% drift, displacement equal to 1% drift and displacements greater than 1% in six cycles, four cycles and two cycles, respectively.

3. 6. Specimen Behavior In the SPSW-1 specimen, by the initiation of the loading, the overall buckling of the web plate in the first mode in 38% drift was observed. Then, as the loading continued, the diagonal tension field began and developed with buckling in the main diagonal of the web plate (with a 53° angle) (Figure 5a).

Then by increasing drifts, the tension field was developed in the entire steel web plate. Slip began earlier and more intensively in the connection of the plate to the boundary element attached to the rigid support.

TABLE 2. Mechanical properties of materials

Sample	Thickness (mm)	Modulus of Elasticity (Gpa)	Poisson Ratio	Yielding Stress (Mpa)	Ultimate stress (Mpa)
Coupon 01	0.8	200	0.3	383	523
Coupon 02	2.95	200	0.3	262	437

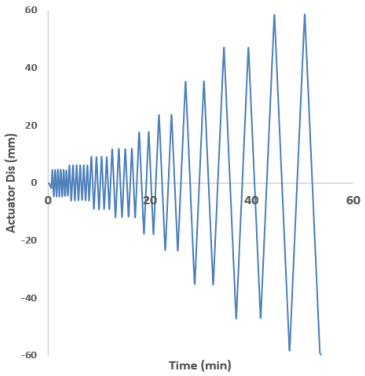

Figure 4. Displacement protocol according to SAC protocol

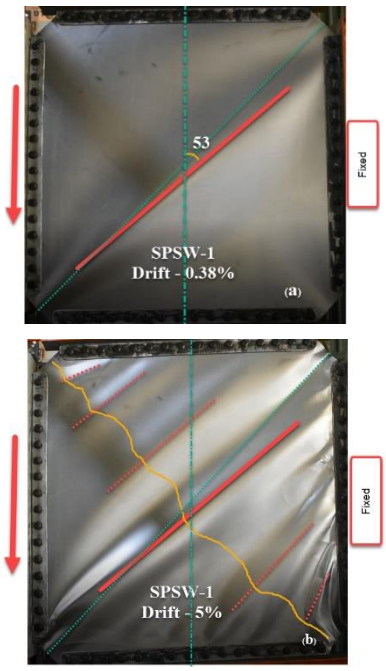

Figure 5. Buckling and the diagonal tension field action; a) diagonal buckling in 0.38% drift, b) development of the tension field in the entire plate at 5% drift

Therefore, at 2% drift, the bolts were tightened again by torque meter. After 4% drift, the diagonal tension field was created in the entire plate with five waves (a wave in the main diagonal and at least two sub-waves on both sides) (Figure 5b). At the end of the loading, severe bearing, cracking and fracture were observed in bolted connection of the web plate (Figure 6). Figure 7 shows the hysteresis curve of the SPSW-1 specimen.

In the butterfly-shaped link specimens, the steel plate was painted with a spray before loading to have a better sight of the buckling location and the beginning of the steel yield. With the beginning of the loading in the SPSW-BL 80 specimen, the compressive buckling of the links on the fixed support side was observed at 0.38% drift in the first loading cycle (Figure 8a) such that

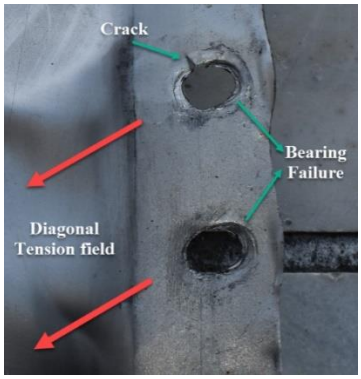

Figure 6. Bearing and fracture in bolted connection

compressive buckling of these links was appeared in the pressure and tension cycles and was removed when the load was reversed. At 2% compressive drift, shear yielding was clearly seen at the critical section of the links (middle section, a) (Figure 8b).

At 3% drift, the lateral-torsional buckling began and as the loading continued, developed in all of the links (Figure 8c). At 5% tensile drift; the topmost link fracture occurred in the boundary element connected to the fixed support in the critical shear section (Figure 8d). Figure 9 shows the beginning of the shear yielding and the fracture of the link.

In the SPSW-BL 130 specimen, the compressive buckling of the links on the side of fixed support occurred in the first loading cycle at 38% drift (Figure 10a), and was removed when the load direction was reversed.

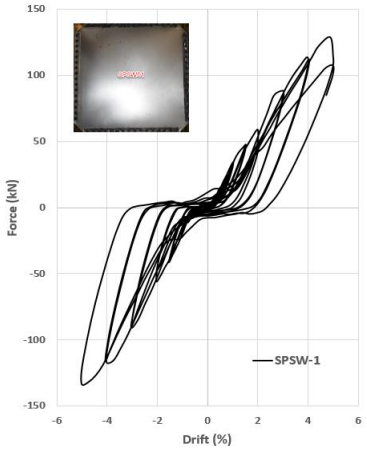

Figure 7. Hysteresis curve of SPSW-1 experimental specimen

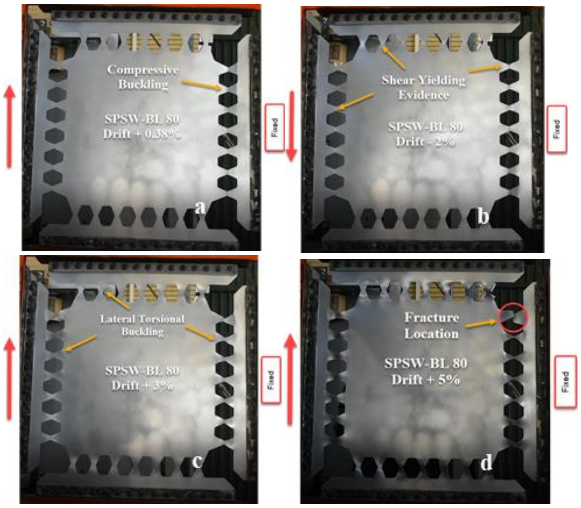

Figure 8. SPSW-BL 80 specimen during loading; a) Compressive buckling at 38% drift, b) The beginning of the shear yielding at 2% compressive drift, c) The beginning of the lateral-torsional buckling at 3% tensile drift, d) fracture of the link at 5% tensile drift

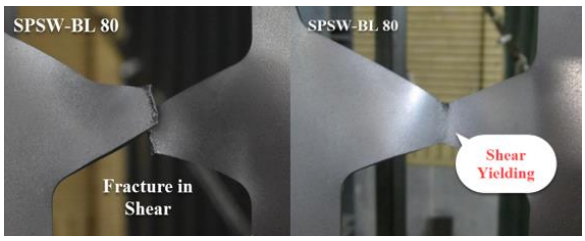

Figure 9. Beginning of the shear yielding and link fracture in SPSW-BL 80 specimen

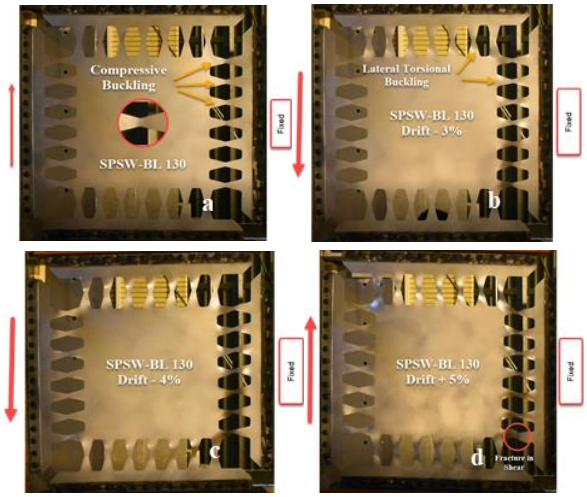

Figure 10. The BL 130 specimen during loading; a) the compressive buckling at 38% drift, b) the start of the shear yielding at 2% drift, c) the beginning of the lateral-torsional buckling at 3% drift, d) fracture of the link at 5% drift

At 3% compressive drift, the lateral-torsional buckling of the links started (Figure 10b) and developed at 4% compressive drift in all links (Figure 10c). At 5% tensile drift, the fracture of the lowest link on the fixed support side occurred at the critical shear section (Figure 10d). Figure 11 shows the fractured link in the BL 130 specimen. The hysteresis curves of BL 80 and BL 130 specimens have been presented in Figure 12.

3. 7. Discussions of Test Results In the SPSW-1 specimen, despite the square shape of the panel, the angle of the tension field in the original diagonal was more than

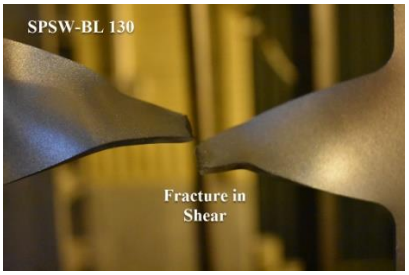

Figure 11. Link fracture in BL 130 specimen

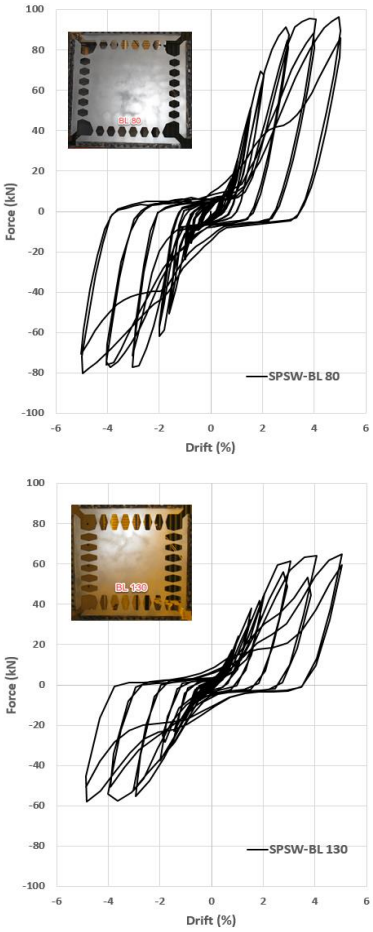

Figure 12. Hysteresis curves for experimental specimens; up) BL 80, down) BL 130

45° (Figure 5a) which was affected by the connection slip on the side of the rigid support. The slip began earlier and more intensively in the plate connection to the boundary element of the fixed support. Despite the slippage, the diagonal tension field was created in the entire web plate within 4% drift. The fracture intensity of bolted connections was observed in the corners, especially on the fixed support side (Figure 6). By examining the hysteresis curve of the SPSW-1 specimen, an intense pinching of the structural system due to the slenderness of the plate and the slip of the joints was observed (Figure 7).

In the SPSW-BL 80 specimen, with the link geometry (a/b=0.33 and b/L=0.62), the shear yielding began before the lateral-torsional buckling of the link and the formation of flexural plastic hinges in L/4 of the middle section of the link [19] at the minimum width (Figure 8b) [22]. Then, with the continuation of the loading, the lateral-torsional buckling occurred in all links. In this specimen, the system's behavior was controlled by the shear limite state. In the SPSW-BL 130 specimen with the link geometry of (a/b=0.33 and b/L=0.38), first, the plastic flexural hinges in the distance of L/4 from the middle section of the link were formed, and then by continuation of the loading, the link experienced shear yielding and fracture in the minimum width, a. In this specimen, the behavior of the system was controlled by flaxural limit state. In both cases, the fracture of the links occurred suddenly and with a sound. By examining the location of the fractured link and other links, It was observed that the compressive buckling of the links in fixed support side has intensified the shear yielding in the middle section of these links. Therefore, the fracture occurred in the critical shear area in the links affected by the compressive buckling in both butterfly-shaped link shear walls despite the difference in the links geometry. However, in both BLSPSW specimens, the load-displacement curves of the specimens were stable with lower pinching and without any strength loss despite the lateral-torsional buckling and even fracture. No bearing and cracking of the plate in bolted connections were observed in the BLSPSW specimens.

3. 7. 1. Stiffness and Strength The ideal bilinear curve for the laboratory specimens is prepared according to FEMA 356 [26] based on the equivalent energy. So, the area under the load-displacement curve (hysteresis envelope curve), and the ideal bilinear curve are equal (Figure 13). The initial stiffness of the structure is an effective parameter in controlling the damage caused by excessive drift of the structure. The stiffness of the specimens is obtained from the ideal bilinear curve according to Equation (3):

$$k = \frac{V_y}{\Delta_y} \quad (3)$$

where V_y and Δ_y, are the equivalent load at the beginning of the yielding and yielding displacement, respectively.

The ultimate strength is obtained directly from the hysteresis curve and equals the maximum load that the specimen bears during loading cycles. Besides, the yield strength is obtained from the ideal bilinear curve as illustrated in Figure 13. The results of initial stiffness and the strength of the specimen are summarized in Table 3. Figure 14 illustrates the ideal bilinear curve for the BL 130 specimen. The initial stiffness of SPSW-1, SPSW-BL 80 and SPSW-BL 130 specimens is 2.55, 2.65, and 1.90 kN/mm, respectively. The stiffness can be adjusted regarding the geometry of the butterfly-shaped links and unlike the conventional walls; the thickness of the plate is not the only factor, which affects the stiffness. In the SPSW-BL 80 (controlled by the shear limit state), the stiffness is greater, and in the SPSW-BL-130 (controlled by the flexure limit state), the stiffness is less than that of the conventional SPSW specimen (SPSW-1).

Table 3 indicates the secondary stiffness of the specimens in which the highest value is for SPSW-1

specimen with 2.26 kN/mm. Yield and ultimate strength in SPSW-1 specimen were 77.50 and 121.20 respectively, indicating an increase of 56 percent after yielding. In sample SPSW-BL 80, the yield and ultimate strength were 79.35 and 88.23, respectively, indicating an 11 percent increase in the strength after yielding. This increase in strength for the SPSW-BL 130, with yield and ultimate strength of 53.40 and 61.40, is about 15 percent. Boundary element sections is controlled by strength.

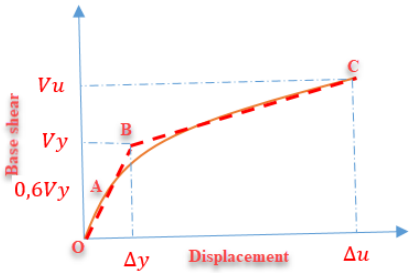

Figure 13. Drawing a bilinear curve in accordance with FEMA 356

TABLE 3. Stiffness and strength results

Sample	Initial Stiffness (kN/mm)		Post Yielding Stiffness (kN/mm)		Yield Strength (kN)		Ultimate Strength (kN)	
	Pos. C.	Neg. C.	Pos. C.	Neg. C.	Pos. C.	Neg. C.	Pos. C.	Neg. C.
SPSW-1	2.45	2.65	2.28	2.25	79.80	75.20	113.70	128.70
	2.55		**2.26**		**77.50**		**121.20**	
BL 80	2.48	2.82	1.37	1.66	71.80	86.90	80.10	96.37
	2.65		**1.52**		**79.35**		**88.23**	
BL 130	1.70	2.11	1.00	1.10	52.00	54.80	57.80	65.00
	1.90		**1.05**		**53.40**		**61.40**	

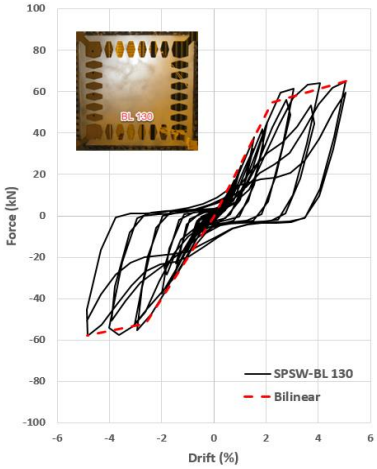

Figure 14. The hysteresis curve of BL 130 specimen and the ideal bilinear curve

The SPSW-BL 80 has a 40, 48 and 44 percent increase in initial stiffness, yield strength, and ultimate strength respectively, in comparison with the SPSW-BL130 which is different only in link geometry. Regardless of the difference in the yielding and ultimate stress of the steel plate materials, the SPSW-BL 80 has a 4 percent greater stiffness and a 27 percent lower ultimate strength in comparison to the SPSW-1.

3. 7. 2. Ductility and Energy Dissipation The capacity of a structure intolerance of displacement after initial yielding, without any drop in the ultimate strength is defined as ductility. The displacement ductility is obtained according to the ideal bilinear curve by Equation (4):

$$\mu = \frac{\Delta_u}{\Delta_y} \quad (4)$$

where Δ_u is the peak plastic displacement of the structure and Δ_y is the yield displacement of the structure (Figure 13).

The overall ductility values of the specimens have been defined based on the extracted results of the ideal bilinear load-displacement curve and presented in Table 4. The displacement ductility values for SPSW-1, SPSW-BL 80 and SPSW-BL 130 specimens have been obtained to be 1.88, 1.95, and 2.07, respectively. Then, the SPSW-BL 80 and SPSW-BL 130 have been about 4 and 10 percent more ductile. Among the proposed walls, the BL 130 was more ductile with the flexural behavior of the link.

The area of each hysteresis loop indicates the amount of dissipated energy during loading. Table 5 shows the amount of energy dissipated at drifts of 1 to 5 percent, as well as the cumulative dissipated energy of the specimens. Up to drift of 3 percent, the energy dissipation values of the BLSPSW specimens are more than SPSW-1. However, with the development of the diagonal tension field and the expansion of yielding into the entire plate, the energy dissipation increases in the SPSW-1 specimen after 4 percent drift ratio. The beginning of the significant energy dissipation at low drift levels is an indication of early shear and flexural yielding in the link regarding its geometry and the optimal performance of the BLSPSW specimens.

TABLE 4. Ductility results

Sample	Yield Disp. (mm)		Ultimate Disp. (mm)		Disp. Ductility		Average Ductility
	Neg. C.	Pos. C.	Neg. C.	Pos. C.	Neg. C.	Pos. C.	
SPSW-1	32.8	28.3	58.4	57.1	1.77	2.00	1.88
BL 80	29	30.8	58.2	57.9	2.00	1.88	1.95
BL 130	30.5	25.9	56.7	59.2	1.85	2.28	2.07

TABLE 5. Energy dissipation results

Sample	Cumulative Energy Dissipation (kN.mm)
SPSW-1	8338.89
BL 80	8409.21
BL 130	6030.40

The cumulative energy dissipation of the SPSW-1 specimen was 8338.89 kN.mm at the end of loading, and for the SPSW-BL 80 and SPSW-BL 130 specimens was obtained to be 8409.21 kN.mm and 6030.40 kN.mm, respectively. Therefore, the total dissipated energy of the proposed system can be higher or lower than SPSW-1 regarding the limit state of the link. The SPSW-BL 80 specimen, has a significant amount of 40 percent more dissipated energy compared to SPSW-BL 130 specimen. Figure 15 indicates the comparison of energy dissipated by experimental specimens at each drift.

4. FINITE ELEMENT ANALYSIS

Nonlinear finite element analysis was used to precisely examine the proposed formula by Farzampour et al. [22] for determination of the butterfly-shaped link capacity. For this purpose, ABAQUS finite element software [27] was used to simulate links. An S4R shell element was used for modeling the butterfly-shaped link which is a four-node element of two curves with reduced integration, and each node of the element has six degrees of freedom (three transitional and three rotational). The link was restrained by fixed support from one side and roller support from the other side that monotonic load was applied to it (Figure 16). First, linear buckling analysis was performed to extract the buckling modes of the butterfly-shaped link, and then a nonlinear analysis with a dynamic explicit solver was used to determine the

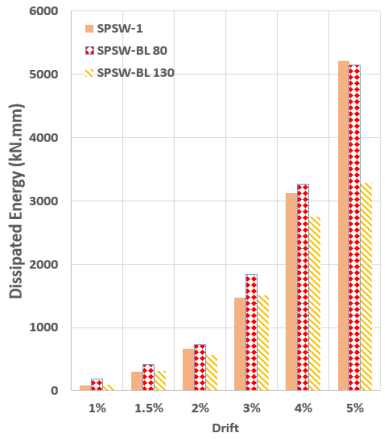

Figure 15. Comparison of energy dissipated by laboratory specimens at each drift

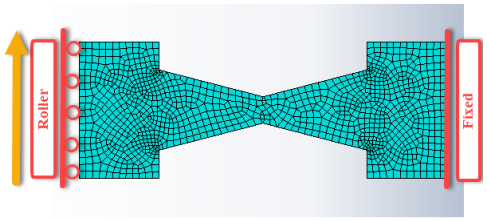

Figure 16. The butterfly-shaped link modeled in Abaqus

link capacity. The initial imperfection was considered, according to the first buckling mode of the link with the maximum out-of-plane displacement in the range of L/250. The specimens were named Link 80 and Link 130 based on the link-length. The geometric properties of the links were considered according to Table 1. The overall length of the specimens in finite element was considered to be L + 100 mm.

In confirmation of the experimental results, the link 80 first experienced the shear yielding (in middle section) at the load of 8.55 kN, and then by forming the flexural plastic hinges, the link capacity reached 12.63 kN (Figure 17). On the contrary, at the link 130, the flexural plastic hinges (at L/4 from the middle section) were initially formed at 5.98 kN, and then with the increase of the load to 10.54 kN, the critical section experienced the shear yielding (Figure 17). In the link 80, with the shear limit state; Equation 2 predicts the shear capacity of the link to be 7.36 kN, which is 14 percent less than the yield capacity derived from the finite element analysis. Also, in the link 130, with flexure limit state, Equation 1a estimates the flexural capacity of the link to be 6.57 kN, which is 9 percent higher than the results of the finite element analysis. By examination of the results, it can be seen that the proposed formula is more precise for the link with the flexural limit state (Link 130).

5. SHEAR STRENGTH PREDICTION

In this section, the strength of experimental specimens of the butterfly-shaped steel plate shear wall (BLSPSWs) is compared with the analytical equations associated with the shear and flexure limit states of the butterfly-shaped links [22] of section 2 (Table 6). Due to the distribution of the internal force of the structural system, the shear capacity of the butterfly-shaped steel plate shear wall is equal to the shear strength of one side links (shear strength of seven links). In the SPSW-BL 80 specimen, the yield strength is 79.35 kN and the ultimate strength is 88.23 kN. Considering the shear yielding as the dominant limit state, shear capacity is obtained to be 50.75 kN by Equation 2 (for n number of links, n= 7). In addition, in the SPSW-BL 130 specimen, the yield strength is 53.40 kN and the ultimate strength is 61.40 kN. Considering the flexural yielding as the dominant limit state of the links,

the specimen capacity is obtained to be 45.30 kN by Equation 1a (for seven links). Therefore, the analytical method for the SPSW-BL 80 and SPSW-BL 130 specimens, estimates the shear capacity of the system 36 percent and 15 percent less than the yield strength of the experimental specimens, respectively. Although, by examining the results of finite element modeling of the links (section 4) and studying the cyclic behavior and fracture modes of BLSPSW specimens in section 3, it seems that choosing the starting points of yielding (both flexural and shear yielding) as the ultimate capacity of the system, especially in the short link specimen (SPSW-BL 80), will be too cautiously.

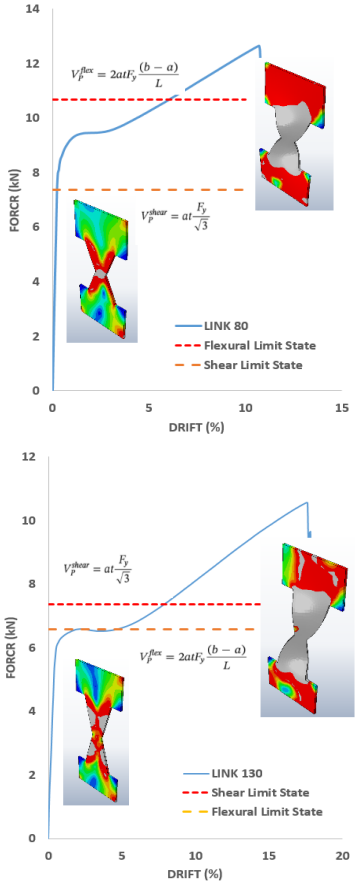

Figure 17. Comparison of analytical results with the results of finite element analysis

TABLE 6. Comparison of experimental and analytical results

Sample	Yield Strength (kN)	Ultimate Strength (kN)	V_P^{flex} Eq. 1a (kN)	V_P^{shear} Eq. 2 (kN)
BL 80	79.35	88.23	73.6	50.75
BL 130	53.40	61.40	45.30	50.75

6. CONCLUSION

In this research, three laboratory specimens were constructed and tested to evaluate the cyclic behavior of the proposed steel plate shear wall with butterfly-shaped links. Also, butterfly-shaped fuses formulation was used to obtain the shear capacity of the proposed steel plate shear wall. The summary of the extracted results is as follows:

The initial stiffness levels of SPSW-1, SPSW-BL 80 and SPSW-BL 130 specimens were 2.55, 2.65 and 1.90 kN/mm, respectively, and the ultimate strengths of the specimens were 121.20, 88.23 and 61.35 kN. Important seismic parameters like initial stiffness and strength of BLSPSW specimens can be controlled by geometric parameters (a/b, L/t and b/L) and the number of links at each side, n. Therefore, in this type of steel plate shear walls, a system with a higher stiffness and lower strength compared to the conventional steel shear walls system can be designed, which can have acceptable and economical boundary elements and controls the drift ratio simultaneously.

SPSW-BL 80 specimen with shear yielding controlled behavior (b/L=0.62) shows 40, 48 and 44 percent increase in the initial stiffness, yield strength and ultimate strength respectively in comparison with the SPSW-BL 130 specimen with controlled behavior of flexural yielding (b/L=0.38).

BLSPSW with shear yielding controlled behavior (SPSW-BL 80) has 4 percent and BLSPSW with flexural yielding controlled behavior (SPSW-BL 130) has 10 percent more ductility compared to SPSW-1 specimen.

The early yield of the links and creation of S-shape hysteresis loops in the small drifts is the superiority of the proposed BLSPSWs structural system compared to the SPSW-1 specimen. However, the increase in the energy dissipation of the SPSW-1 specimen intensified after 4 percent drift with the complete yield of the plate.

The cumulative energy dissipation of SPSW-1, SPSW-BL 80 and SPSW-BL 130 specimens at the end of loading were 8338.89, 8409.21, and 6030.40 kN.mm, respectively. Therefore, the dissipated energy of the proposed system can be greater or lower than the conventional wall specimen (SPSW-1) concerning the limit state that controls the link behavior.

The SPSW-BL 80 specimen has a higher energy dissipation of 40 percent compared to the SPSW-BL 130 specimen.

High slip, bearing, and fracture of the SPSW-1 specimen was observed at the end of loading in the bolted connection of the plate to the boundary elements. BLSPSW specimens also experienced a fracture of one link at 5 percent ratio. However, the link fracture did not affect the stable behavior of the hysteresis curve of the specimens and the reduction of the system's strength. In

BLSPSW specimens, bearing and fracture were not observed in bolted connections.

Analytical formulation estimates the shear capacity of SPSW-BL 80 and SPSW-BL 130 specimens to be 36 and 15 percent lower than the yield strength of the experimental results. Therefore, choosing the starting points of yielding (flexural or shear yielding) as the ultimate capacity of the system, especially in links with shear yield limit state, will be too cautiously.

7. REFERENCES

1. Thorburn, L.J., Montgomery, C.J. and Kulak, G.L., Analysis of steel plate shear walls, Structural Engineering, Report No. 107, Edmonton (AB): University of Alberta, (1983).
2. Lubell, A.S., Prion, H.G., Ventura, C.E. and Rezai, M., "Unstiffened steel plate shear wall performance under cyclic loading", ***Journal of structural Engineering***, Vol. 126, No. 4, (2000), 453–460.
3. Qu, B. and Bruneau, M., "Design of steel plate shear walls considering boundary frame moment resisting action", ***Journal of Structural Engineering***, Vol. 135, No. 12, (2009), 1511–1521.
4. Basler, K., "Strength of plate girders in shear", ***Journal of the Structural Division***, Vol. 87, No. 7, (1961), 151–180.
5. Caccese, V., Elgaaly, M. and Chen, R., "Experimental study of thin steel-plate shear walls under cyclic load", ***Journal of Structural Engineering***, Vol. 119, No. 2, (1993), 573–587.
6. Elgaaly, M., "Thin steel plate shear walls behavior and analysis", ***Thin-Walled Structures***, Vol. 32, No. 1–3, (1998), 151–180.
7. Sabelli, R. and Bruneau, M., Design guide 20: steel plate shear walls, American Institute of Steel Construction (AISC), (2007).
8. Berman, J.W. and Bruneau, M., "Capacity design of vertical boundary elements in steel plate shear walls", ***Engineering Journal,*** AISC, First Quarter, (2008), 57–71.
9. AISC, Seismic provisions for structural steel buildings, American Institute of Steel Construction (AISC), ANSI/AISC 341-16, Chicago, (2002).
10. Roberts, T.M. and Sabouri-Ghomi, S., "Hysteretic characteristics of unstiffened perforated steel plate shear panels", ***Thin-Walled Structures***, Vol. 14, No. 2, (1992), 139–151.
11. Valizadeh, H., Sheidaii, M. and Showkati, H., "Experimental investigation on cyclic behavior of perforated steel plate shear walls", ***Journal of Constructional Steel Research***, Vol. 70, (2012), 308–316.
12. Berman, J.W. and Bruneau, M., "Experimental investigation of light-gauge steel plate shear walls", ***Journal of Structural Engineering***, Vol. 131, No. 2, (2005), 259–267.
13. Chen, S.J. and Jhang, C., "Cyclic behavior of low yield point steel shear walls", ***Thin-Walled Structures***, Vol. 44, No. 7, (2006), 730–738.
14. Hitaka, T. and Matsui, C., "Experimental study on steel shear wall with slits", ***Journal of Structural Engineering***, Vol. 129, No. 5, (2003), 586–595.
15. Hitaka, T., Matsui, C. and Sakai, J. I., "Cyclic tests on steel and concrete-filled tube frames with Slit Walls", ***Earthquake Engineering & Structural Dynamics***, Vol. 36, No. 6, (2007), 707–727.
16. Choi, I.R. and Park, H. G., "Steel plate shear walls with various infill plate designs", ***Journal of Structural Engineering***, Vol. 135, No. 7, (2009), 785–796.
17. Liu, Q., Li, G.Q. and Lu, Y., "Experimental and theoretical study on the steel bound-columns with buckling restrained steel plate shear wall", In Proceedings of the EUROSTEEL, 7th European Conference on Steel and Composite Structures, Italy, (2014).
18. Jin, S., Ou, J. and Liew, J. R., "Stability of buckling-restrained steel plate shear walls with inclined-slots: theoretical analysis and design recommendations", ***Journal of Constructional Steel Research***, Vol. 117, (2016), 13–23.
19. Ma, X., Borchers, E., Pena, A., Krawinkler, H., Billington, S. and Deierlein, G. G., "Design and behavior of steel shear plates with openings as energy-dissipating fuses", Report No. 173: The John A. Blume Earthquake Engineering Center, (2010).
20. Eatherton, M.R., Ma, X., Krawinkler, H., Deierlein, G.G. and Hajjar, J. F., "Quasi-static cyclic behavior of controlled rocking steel frames", ***Journal of Structural Engineering***, Vol. 140, No. 11, (2014), 04014083(1–11).
21. El-Bahey, S. and Bruneau, M., "Bridge piers with structural fuses and bi-steel columns. I: Experimental testing", ***Journal of Bridge Engineering***, Vol. 17, No. 1, (2011), 25–35.
22. Farzampour, A. and Eatherton, M. R., "Yielding and lateral torsional buckling limit states for butterfly-shaped shear links", ***Engineering Structures***, Vol. 180, (2019), 442–451.
23. Farzampour, A. and Eatherton, M. R., "Lateral torsional buckling of butterfly-shaped shear links", In Proceedings of the SSRC Annual Stability Conference Structural Stability Research Council, San Antonio, USA, (2017), 21–24.
24. ASTM, "Standard test methods for tension testing of metallic materials", ASTM E8/E8M-09. West Conshohocken, PA: ASTM, (2009).
25. SAC Joint Venture, "Protocol for fabrication, inspection, testing, and documentation of beam-column connection tests and other experimental specimens", Report No. SAC/BD-97/02, Federal Emergency Management Agency: Washington, (1997).
26. FEMA, "Prestandard and commentary for the seismic rehabilitation of buildings", Federal Emergency Management Agency, American Society of Civil Engineers (ASCE), Report FEMA-356, Washington, (2000).
27. ABAQUS/CAE, "Dassault Systemes Simulia Corporation", (2018).

Experimental Investigation on Cyclic Behavior of Butterfly-shaped Links Steel Plate Shear Walls

H. Valizadeh[a], H. Veladi[a], B. Farahmand Azar[a], M. R. Sheidaii[b]

[a] *Civil Engineering Faculty, Tabriz University, Tabriz, Iran*
[b] *Civil Engineering Department, Urmia University, Urmia, Iran*

P A P E R I N F O

Paper history:
Received 10 July 2019
Received in revised form 05 September 2019
Accepted 12 September 2019

Keywords:
Butterfly Link
Energy Dissipation
Ductility
Shear Capacity
Steel Plate Shear Wall

چکیده

تیپ نوآورانه‌ای تحت عنوان دیوار برشی فولادی لینک پروانه‌ای شکل (BLSPSW) بعنوان سیستم باربر جانبی پیشنهاد شد. در این سیستم با ایجاد لینک‌های پروانه‌ای شکل محیطی در چهار ضلع ورق جان، مکانیزم باربری جانبی مشابه دیوارهای برشی فولادی متعارف، توسعه میدان کشش قطری در ورق جان نبوده، بلکه ظرفیت سیستم با مقاومت برشی لینک‌ها تعیین می‌گردد. بنابراین، پارامترهای هندسی لینک بعنوان ورودی اولیه طراحی در پیش‌بینی و کنترل سختی و مقاومت سیستم سازه‌ای اثرگذار می‌باشند. برای بررسی رفتار سیستم پیشنهادی سه نمونه آزمایشگاهی تهیه و بارگذاری شد. نمونه اول دیوار برشی فولادی متعارف (SPSW-1)، و دو نمونه دیگر دیوار برشی فولادی لینک پروانه‌ای شکل (BLSPSW) با رفتار لینک‌های کنترل‌شده با تسلیم برشی (BL 80) و کنترل‌شده با تسلیم خمشی (BL 130) تهیه شد. نتایج آزمایشگاهی نشان‌دهنده قابلیت کنترل سختی و مقاومت نمونه‌های پیشنهادی با کنترل هندسه لینک، شکل‌پذیری مطلوب تا ۱۰ درصد بیشتر، استهلاک انرژی بالا بویژه شروع استهلاک انرژی قابل‌توجه در دریفت‌های کوچک در چرخه‌های هیسترزیس، نسبت به نمونه SPSW-1 بود. در انتها فرمول‌بندی مقاومت برشی لینک‌های پروانه‌ای شکل برای تعیین ظرفیت سیستم پیشنهادی بکار رفت و با نتایج آزمایشگاهی مقایسه شد.

***doi**: 10.5829/ije.2019.32.11a.07*